凹凸 反射器에서 表面波의 解析

○송 준 태 H.F. Tiersten
성균관대학교 전기공학과 Rensselaer Polytechnic Institute

THE ANALYSIS OF THE SURFACE WAVES BY ARRAYS OF REFLECTING GROOVES

J. T. Song H.F. Tiersten
Department of Electrical Eng. Sung Kyun Kwan Univ. Rensselaer Polytechnic Institute

1. Introduction

Previous variational analyses of the reflection of surface waves were for arrays of reflecting strips. In this work a variational analysis of the reflection of surface waves by arrays of reflecting grooves is presented. The variational condition results in a system of linear algebraic eqations relating the amplitudes of the waves on both sides of the edge of a groove. The straight-created surface wave velocity is taken to be the same on both sides of the edge of a groove. When the phase of the reflected wave has been found, the resonant frequency and associated phase velocity of the standing surface wave mode is obtained from a perturbation eqation. Calculated results are presented for grooved arrays on ST-cut quartz and, in particular, it is shown that the calculated reduced phase velocities are in good agreement with measurements of Tanski.

2 Preliminary Considerations

A cross-section of a typical portion of the grooved array is shown in Fig.1 along with the coordinate system, which shows that the x-axis(x_1=0) is at the mean surface of the grooved array since $dh_1=lh_2$. This mean surface is the surface from which the unperturbed surface wave mode is perturbed due to the grooved surface geometry to produce a change in phase velocity. The solusion for straight-created propagating surface waves may be written in the form,

$$u_j = \sum_{m=1}^{4} C^{(m)} A_j^{(m)} e^{i\beta_m^{(m)} x_2} e^{i\xi(x_1-Vt)},$$
$$\varphi = \sum_{m=1}^{4} C^{(m)} A_4^{(m)} e^{i\beta_m^{(m)} x_2} e^{i\xi(x_1-Vt)} \qquad (1)$$

where the $C^{(m)}$, $A_j^{(m)}$, $A_4^{(m)}$, $\beta^{(m)}$ and V are determinated so that the differential equations and boundary conditions are satisfied. The equation for the perturbation in phase velocity is given by

$$\Delta V = -H_1/2V_1\xi^2, \quad \Delta V = V - V_1, \qquad (2)$$

where V_1 and V are the unperturbed and perturbed phase velocities respectively, and

$$H_1 = \int_S n_i (T_{ij} g_j^1 - u_j T_{ij}^1)\, dS, \qquad (3)$$

in which the electric terms have been omitted because of small piezoeletric coupling and the normalized mechanical displacement g_j^1 is defined by

$$g_j^1 = u_j/N_1, \quad N_1^2 = \int_V \rho u_j u_j\, dV, \qquad (4)$$

and T_{ij}^1 is the associated stress tensor.
Futhermore, in (3) u_j and T_{ij} are the actual, i.e., perturbed displacement vector and stress tensor, respectively, and n_i denotes the outwardly directed unit normal to the surface of the grooved array. Since in the case considered here we perturbed from the mean surface to the grooved surface shown in fig.1, $n_i T_{ij}=0$ in (3), which then reduces to

$$H_1 = -\int_S n_i T_{ij}^1 u_j\, dS. \qquad (5)$$

Accordingly, application of (5) to the grooved array shown in Fig.1 over a typical wavelength at resonance yields

$$\begin{aligned} H_1 = &\int_0^d u_j T_{2j}|_{x_2=-h_1}\, dx_1 - \int_{-h_1}^{h_2} u_j T_{1j}|_{x_1=d}\, dx_2 \\ &+ \int_d^{d+\ell} u_j T_{2j}|_{x_2=-h_2}\, dx_1 + \int_{-h_1}^{h_2} u_j T_{1j}|_{x_1=d+\ell}\, dx_2 \\ &+ \int_d^{d+\ell} u_j T_{2j}|_{x_2=-h_1}\, dx_1 - \int_{-h_1}^{h_2} u_j T_{1j}|_{x_1=2d+\ell}\, dx_2 \\ &+ \int_{2d+\ell}^{2(d+\ell)} u_j T_{2j}|_{x_2=-h_2}\, dx_1 + \int_{-h_1}^{h_2} u_j T_{1j}|_{x_1=2(d+\ell)}\, dx_2 . \end{aligned} \qquad (6)$$

3. Variational Analysis of Edge of Groove

We expend $u_j(x_1,x_2,t)$ and $\varphi(x_1,x_2,t)$ as mentioned above in the form

$$u_j = \alpha_j(x_2)\psi(x_1), \quad \varphi = \alpha_4(x_2)\psi(x_1), \qquad (7)$$

in which we have suppressed the time dependence $e^{-i\omega t}$ and where

$$(\alpha_j,\alpha_4) = \sum_{m=1}^{4} C^{(m)}(A_j^{(m)},A_4^{(m)})e^{i\beta_m \xi x_2}, \qquad (8)$$

as is known from (1) and we note that for a negative traveling wave we must replace (α_j,α_4) in (8) by (α_j^*,α_4^*). Since we have assumed only surface waves which satisfy the differential equations and boundary conditions on the surfaces $\eta_i = (0, -1, 0)$ all that remains of the variational principle of linear piezoelectricity, or rather for small coupling, linear electricity, is

$$\int_0^{\infty} T_{1j}\delta u_j dx_2 = \int_{2h}^{\infty} \bar{T}_{1j}\delta \bar{u}_j dx_2, \qquad (9)$$

4. Transmission Equations for the Reflecting Array

The surface wave solution functions for the three consecutive sections may be written in the form

$$\begin{aligned}
\hat{\phi}_n &= \left[C_n^R e^{i\xi(x_1-z_n+d)} + C_n^L e^{-i\xi(x_1-z_n+d)}\right] e^{-i\omega t},\\
\hat{\bar{\phi}}_{n+1} &= \left[\bar{C}_{n+1}^R e^{i\xi(x_1-z_n)} + \bar{C}_{n+1}^L e^{-i\xi(x_1-z_n)}\right] e^{-i\omega t}, \qquad (10)\\
\hat{\phi}_{n+1} &= \left[C_{n+1}^R e^{i\xi(x_1-z_n-\ell)} + C_{n+1}^L e^{-i\xi(x_1-z_n-\ell)}\right] e^{-i\omega t},
\end{aligned}$$

where

$$z_n = n(\ell+d), \qquad (11)$$

and c_m^R and c_m^L denote the amplitudes of the waves traveling to the right and left, respectively, in the mth section. Substituting from (10) into the junction conditions at $x_1=z_m$ and $x_1=z_m+\ell$ and eliminating the $\bar{C}_{n+1}^R$ and $\bar{C}_{n+1}^L$, we obtain the transmission equations

$$\begin{pmatrix} C_{n+1}^R \\ C_{n+1}^L \end{pmatrix} = \begin{pmatrix} T_{11} & T_{12} \\ T_{21} & T_{22} \end{pmatrix} \begin{pmatrix} C_n^R \\ C_n^L \end{pmatrix}, \qquad (12)$$

where the transmission matrix T is given by

$$\begin{aligned}
T_{11} &= \{(M^*-\bar{M})(\bar{M}^*-M)\exp[i(\xi\ell+\xi d)] + (M^*-\bar{M}^*)\\
&\quad\times (M-\bar{M})\exp[i(\xi d-\xi\ell)]\}[(M^*-M)(\bar{M}^*-\bar{M})]^{-1},\\
T_{12} &= \{(M^*-\bar{M})(\bar{M}^*-M^*)\exp[i(\xi\ell-\xi d)] + (M^*-\bar{M}^*)\\
&\quad\times (M^*-\bar{M})\exp[-i(\xi\ell+\xi d)]\}[(M^*-M)(\bar{M}^*-\bar{M})]^{-1},\\
T_{21} &= \{(M-\bar{M})(M-\bar{M}^*)\exp[i(\xi\ell+\xi d)] + (M-\bar{M}^*)(\bar{M}-M)\\
&\quad\times \exp[i(\xi d-\xi\ell)]\}[(M^*-M)(\bar{M}^*-\bar{M})]^{-1},\\
T_{22} &= \{(\bar{M}-M)(\bar{M}^*-M^*)\exp[i(\xi\ell-\xi d)] + (\bar{M}^*-M)\\
&\quad\times (M^*-\bar{M})\exp[-i(\xi\ell+\xi d)]\}[(M^*-M)(\bar{M}^*-\bar{M})]^{-1},
\end{aligned} \qquad (13)$$

and

$$\begin{aligned}
M &= i\xi(c_{11}H_{11}+e_{11}H_{41}+c_{56}H_{32}+c_{66}H_{22}+c_{55}H_{33}\\
&\quad + c_{56}H_{23})+c_{12}H_{2,21}+c_{14}H_{3,21}+c_{66}H_{1,22}+\\
&\quad + e_{26}H_{4,22}+c_{56}H_{1,23}+e_{25}H_{4,23},
\end{aligned} \qquad (14)$$

for the ungrooved region and there are bars on the appropriate quantites for the grooved region. From (13) it can be seen that the matrix T has the very important properties

$$T_{21} = T_{12}^*, \quad T_{22} = T_{11}^*. \qquad (15)$$

5. Continuous Representation Along the Transmission Path

The amplitudes of the transmitted and reflected waves may take the form

$$\begin{aligned}
C_o^L &= \frac{r_1 r_2}{b}(e^{-\alpha_1 N} - e^{-\alpha_2 N})\bar{C},\\
C_N^R &= \frac{(r_1-r_2)}{b} e^{-(\alpha_1+\alpha_2)N} e^{iN\pi}\bar{C}.
\end{aligned} \qquad (16)$$

The power reflection and power transmission coefficients R_p and T_p, respectively defined by

$$\begin{aligned}
R_p &= 10\log_{10}(C_o^L C_o^{L*}/\bar{C}\bar{C}^*),\\
T_p &= 10\log_{10}(C_N^R C_N^{R*}/\bar{C}\bar{C}^*),
\end{aligned} \qquad (17)$$

may now readily be caculated for a given configuration and a given number of grooves. Such caculations have been performed for a particular configuration consisting of 300 grooves 759 Å deep on an ST-cut quartz substrate with $l/d=.53/.47$, which results in a surface wave resonator with a fundamental resonant frequency of 400 MHz. The results of the calculations are plotted in Figs.4 and 5, both of which are indistinguishable from the results obtained by cascading the transmission matrix. The amplitude and power reflection coefficients for the same geometric arrangement of grooves, but for a varying number N have been calculated at the center frequency of 400 MHz and are plotted in Fig.6.

Such calculations have been performed for a range of l/d between 1 and $.55/.45$ and the results are plotted in Fig.7 along with experimental data due to Tanski. The calculated results consist of a sequence of the straight line, one for each l/d ratio. The figure seems to indicate that the resonators used in Tanski experiments had slight variations in l/d ratio and that they were closer to $l=d$ for smaller groove depths. At resonance we very accurately have

$$\phi = \left[\hat{C}^R(x_1)e^{i\xi x_1} + \hat{C}^L(x_1)e^{-i\xi x_1}\right] e^{-i\omega t}, \qquad (18)$$

throughout the entire array. Consequently, from (6), (7) and (18) the entire surface wave mode shape may be written in the form

$$\begin{aligned}
\hat{u}_j &= \cos \nu x_3 \,\mathrm{Re}\,\alpha_j(x_2)\left[\hat{C}^R(x_1)e^{i\xi x_1}\right.\\
&\quad \left. + \hat{C}^L(x_1)e^{-i\xi x_1}\right] e^{-i\omega t},
\end{aligned} \qquad (19)$$

In (19) it must be remembered that while α_j goes with ξ, α_j^* goes with $-\xi$ by virtue of (8) and the fact that the surface wave must decay with x_2. Equations (19)

may be employed in a perturbation integral along with a biasing state to calculate a change in resonant frequency of a surface wave resonator.For the surface wave resonator considered in Fig.4 and 5 the standing surface wave mode shapes along the transmission path for the phases $\sin\omega t$ and $\cos\omega t$ have been calculated at resonance and are plotted in Figs.8 and 9, respectively. It can be seen from the figures that the standing surface wave mode shape at resonance has essentially zero phase throughout the array and that the $\sin\omega t$ term can be seen at all only near the front end of the array where the mode is largest; This small $\sin\omega t$ term arises because a small amount of power is transmitted at resonance.

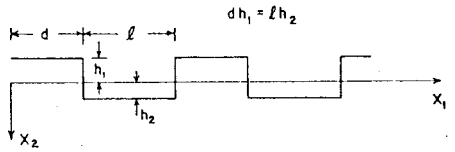

Figure 2. Cross-Ssction of Typical Portion of the Grooved Array for the Variational Analysis of the Edge of a Groove

References

1. B.K. Sinha and H.F. Tiersten, "A Variational Analysis of the Reflection of Surface Waves by Arrays of Reflecting Strips,"J. Appl. Phys., 47, 2824(1976).

2. B.K. Sinha and H.F. Tiersten, "An Analysis of Transverse Modes in Acoustic Surface Wave Resonators,"J. Appl.Phys.,51,3099(1980).

3. W.J. Tanski, "Developments in Resonators in Quartz,"1977 Ultrasonics Symposium Proceedings, IEEE Cat. No. 77 CH 1264-1SU (Institute of Electrical and Electronics Engineers,New York, 1977), p.900.

4. J.J. Campbell and W.R.Jones, "A Method for Estimating Optimal Crystal Cuts and Propagation Directions for Exitation of Piezoelectric Surface Waves," IEEE Trans. Sonics Ultrason.,SU-15,(1968).

5. H. F. Tiersten, J.T. Song and D.V. Shick," A Variational Analysis of the Reflection of Surface Waves by Arrays of Reflecting Grooves,"Proceedings of the 1986 IEEE Ultrasonic Symposium.

6. H. F. Tiersten, J. T. Song, and D. V. Shick,"On a Continuous Representation of the Acoustic Surface Wave Mode Shape in Arrays of Reflecting Grooves," Technical Report,Rensselaer Polytechnic Institute (1986)

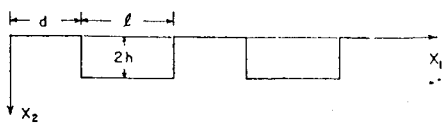

Figure 1. Cross-Section of Typical Portion of the Grooved Array for the Perturbation Analysis

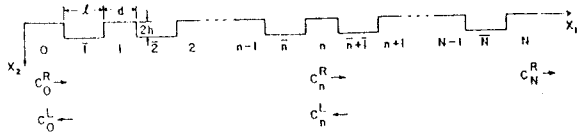

Figure 3. Cross- Section of a Grooved Array Surface-Wave Reflector

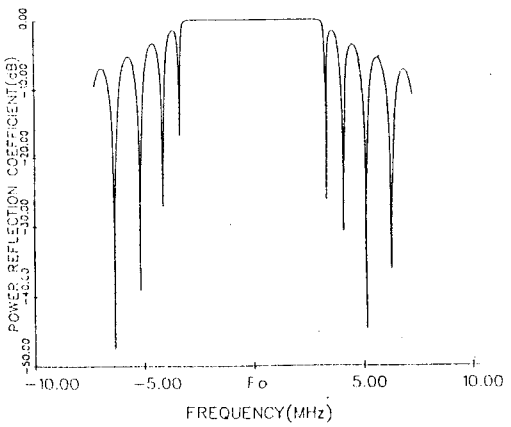

Figure 4. Power Reflection Coefficient of a Surface-Wave Reflector with 300 Grooves 759 Å Deep on ST- Cut Quartz at a Fundamental Frequency of 400 MHz. Results are for 1/d=.53/.47 and 2w=100λ

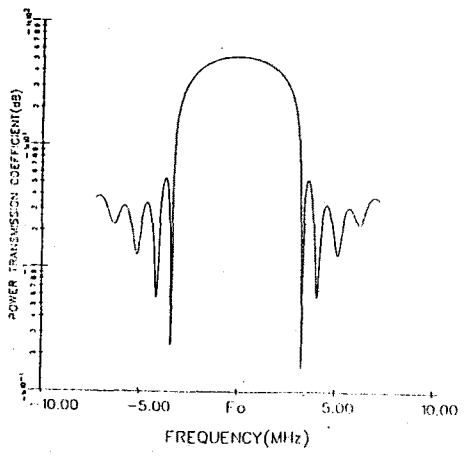

Figure 5. Power Transmission Coefficient of the Grooved Surface-Wave Reflector

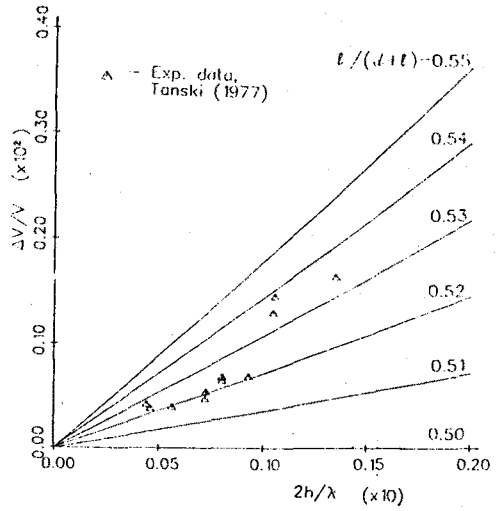

Figure 7. Relative Reduction in the Surface Wave Phase Velocity of the Resonant Mode

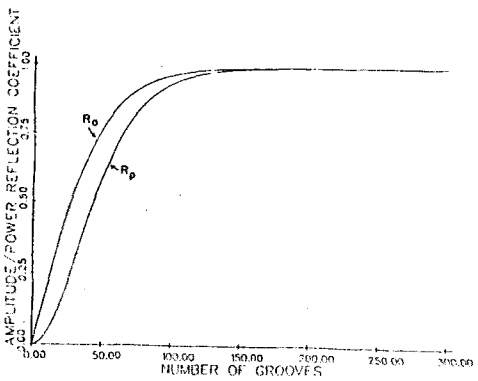

Figure 6. Amplitude (R_α) and Power (R_p) Reflection Coefficients of the Surface-Wave Reflector with Grooves 759 Å Deep at a Center Frequency of 480MHz, as a Function of the Number of Grooves

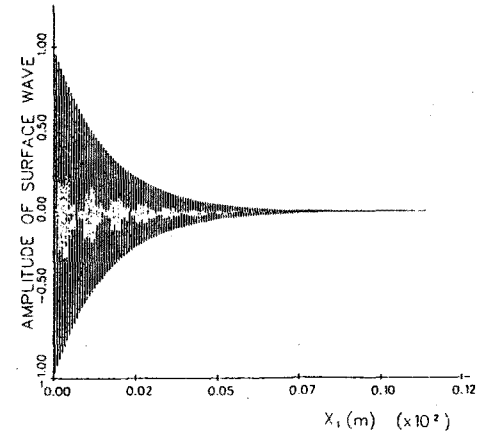

Figure 8. Standing Surface Wave Mode Shape Along Transmission Path at Resonance

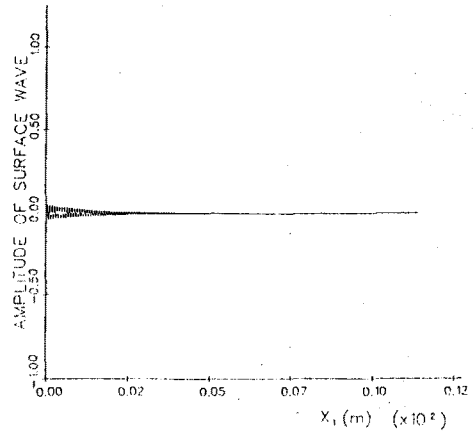

Figure 9. Out of Phase Mode Shape